

## ANALYSIS OF UNDULAR FREE-SURFACE TRANSITIONAL FLOWS

Oscar Castro Orgaz

*Instituto de Agricultura Sostenible, Consejo Superior de Investigaciones Cientificas*

Jose Luis Ayuso Muñoz

*Dept. of Rural Engineering, University of Cordoba*

Juan Vicente Giráldez Cervera

*Dept. of Agronomy University of Cordoba*

### Abstract

Project engineering in water resources management specifically involves free surface flows in open channels systems. Typical channel control design includes the project of gates and weirs for both discharge measurement and water level control. Current design practice for real projects, however, rely on the use of commercial codes based on the gradually-varied flow theory, as, for example, *HEC-RAS*. However, this modeling approach is not accurate in many real cases. Under some circumstances the flow conditions deviate from the gradually-varied flow theory, and the real operational conditions results in dangerous undular free surface flows changing from subcritical to supercritical flow, and vice-versa. These flows are highly different from the assumed standard open channel hydraulics in commercial general codes. In this study an advanced hydraulic modeling approach is proposed for the analysis of undular free surface flow past gates and weirs. The model is successfully verified with experimental data. The solution is detailed, permitting its adoption for design purposes in water resources project engineering practice.

**Keywords:** *Frictional effects; hydraulic jump; transitional flow; turbulence; undular flow*

### Resumen

La ingeniería de proyectos de recursos hidráulicos esta relacionada con el diseño y funcionamiento de las obras hidráulicas presentes en los proyectos de ingeniería civil. El diseño típico de las estructuras de control de canales incluye el proyecto de compuertas y de vertederos para la medida del caudal y el control del nivel del agua. En la práctica profesional la fase de diseño en los proyectos suele basarse en el uso de códigos comerciales, como por ejemplo *HEC-RAS*, que usan la teoría de flujo gradualmente variado en canales abiertos. Esta aproximación hidráulica no es adecuada en muchos casos reales en los que las condiciones del flujo se desvían de la teoría del flujo gradualmente variado, y el funcionamiento de vertederos y compuertas implica de forma peligrosa flujos ondulatorios, donde el flujo cambia de régimen. Un modelo hidráulico más general se requiere en estos casos. En este estudio se propone un modelo hidráulico avanzado para describir el flujo ondulatorio en compuertas y vertederos. El modelo ha sido verificado de forma satisfactoria con datos experimentales. La solución propuesta se presenta en detalle, permitiendo su uso para el diseño de estructuras hidráulicas en la práctica profesional de proyectos.

**Palabras clave:** *Cambio de régimen; efectos de fricción; flujo ondulatorio; resalto hidráulico; turbulencia*

## 1. Introduction

Engineering projects in water resources management are frequently based on the design of free surface open channel systems with transitions across the critical depth caused by the operation of control structures as gates and weirs. Current practice, however, is usually supported by the use commercial codes like HEC-RAS based on gradually-varied flow theory, which fails to reproduce the transitional flow across the critical depth. Open channel flow near the critical depth is characterized by the appearance of steady free surface undulations. Two of the most relevant types of near critical flows are the undular hydraulic jump and the undular weir flow (Chanson, 1996). The undular hydraulic jump is a transition from supercritical ( $F > 1$ ) to subcritical ( $F < 1$ ) flow in the form of steady waves, typically if  $F_1$ , the approach Froude number, is close to unity. Fawer (1937) was the first author that analyzed this problem from a fundamental approach, although it was earlier observed by Darcy and Bazin in 1865. Fawer treated undular hydraulic jumps with a Boussinesq-type energy equation (Castro-Orgaz, 2009). He did not consider the transition from  $F > 1$  to  $F < 1$  before the first wave crest, but reported the undular flow features in carefully designed experiments. Many authors studied the undular jump using the potential flow theory (Fawer, 1937; Iwasa, 1955; Mandrup-Andersen, 1978), but only Montes (1986) and Montes and Chanson (1998) explicitly discussed the importance of wall friction, incorporating the real fluid flow characteristics. The undular weir flow is a transition from subcritical ( $F < 1$ ) to supercritical ( $F > 1$ ) flow in the form of steady waves, typically if  $H_o/L < 0.15$  (Montes, 1998), with  $H_o$  as the upstream head on the weir and  $L$  as the crest length. Flow over broad-crested weirs for  $H_o/L < 0.5$  is usually modeled by a parallel-streamline flow approach (Harrison, 1967). Nevertheless the free surface undulations appearing on the weir crest for  $H_o/L < 0.15$  invalidate this treatment.

In this paper, the undular hydraulic jump and the undular weir flow are analyzed with an approximate model derived from the Reynolds equations for turbulent free surface flows. The results are compared with experimental data and a good agreement was found.

## 2. Governing equations

The time-averaged velocity  $\bar{u}$  parallel to the channel bottom in steady two-dimensional free surface flow may be approximated to the lowest order by its depth-averaged value  $U$

$$\bar{u} = U = \frac{q}{h} \quad (1)$$

The unit discharge is  $q$  and  $h$  is the flow depth. Using the time-averaged form of the 2D continuity equation

$$\frac{\partial \bar{u}}{\partial x} + \frac{\partial \bar{v}}{\partial y} = 0 \quad (2)$$

the time-averaged velocity  $\bar{v}$  normal to the channel bottom is, after integration,

$$\bar{v} = -\int_0^y \frac{\partial U}{\partial x} dy = Uh'\eta \quad (3)$$

In equation (3)  $h'$  represents the derivative of the flow depth with respect to the streamwise coordinate along the channel bottom,  $x$ ,  $h' = dh/dx$ , and  $\eta = y/h$ . The time-averaged momentum balance perpendicular to the channel bottom is

$$\bar{u} \frac{\partial \bar{v}}{\partial x} + \bar{v} \frac{\partial \bar{v}}{\partial y} = -\frac{1}{\rho} \frac{\partial \bar{p}}{\partial y} - \frac{1}{\rho} \frac{\partial \overline{u'v'}}{\partial x} - g \cos \alpha \quad (4)$$

where the time-averaged pressure is  $\bar{p}$ ,  $\tau = -\overline{u'v'}$  is the tangential turbulent Reynolds stress, and  $\alpha$  the angle of the channel bottom with respect to the horizontal plane. The convective acceleration term in equation (4) can be written using equation (2) as

$$\bar{u} \frac{\partial \bar{v}}{\partial x} + \bar{v} \frac{\partial \bar{v}}{\partial y} = \bar{u}^2 \frac{\partial}{\partial x} \left( \frac{\bar{v}}{\bar{u}} \right) \quad (5)$$

Inserting equations (1), (3) and (5) into equation (4), and noting that  $\partial \tau / \partial x \ll \partial \bar{p} / \partial y$ , its integration yields

$$\frac{\bar{p}}{\gamma} = (h - y) \cos \alpha + \frac{U^2}{2g} (hh'' - h'^2) [1 - \eta^2] \quad (6)$$

In the last equation  $h'' = d^2h/dx^2$ . Equation (6) gives the pressure distribution in wavy 2D free surface flows (Serre, 1953; Montes, 1986, 1998). It is worth pointing out that equation (6) was obtained from the assumptions that: (i) the x-direction velocity distribution may be approximated by its depth-averaged value  $\bar{u} = q/h$ , a reasonable approximation for Reynolds numbers  $R \rightarrow \infty$ ; (ii) turbulence shear stresses are dominant in the y-direction,  $\partial \tau / \partial x \ll \partial \tau / \partial y$ . Therefore equation (6) is not limited to irrotational flows as it is the case in other Boussinesq-type developments based on a potential flow approach (Marchi, 1963; Matthew, 1963, 1991).

The time-averaged momentum balance in the x-direction is

$$\bar{u} \frac{\partial \bar{u}}{\partial x} + \bar{v} \frac{\partial \bar{u}}{\partial y} = -\frac{1}{\rho} \frac{\partial \bar{p}}{\partial x} - \frac{1}{\rho} \frac{\partial \overline{u'v'}}{\partial y} + g \sin \alpha \quad (7)$$

Using equations (1), (3) and

$$\bar{u} \frac{\partial \bar{u}}{\partial x} + \bar{v} \frac{\partial \bar{u}}{\partial y} = \frac{\partial \bar{u}^2}{\partial x} + \frac{\partial \bar{u}\bar{v}}{\partial y} \quad (8)$$

with equation (7) leads to

$$\frac{\partial \bar{u}^2}{\partial x} + \frac{\partial \bar{u}\bar{v}}{\partial y} = -\frac{1}{\rho} \frac{\partial \bar{p}}{\partial x} - \frac{1}{\rho} \frac{\partial \overline{u'v'}}{\partial y} + g \sin \alpha \quad (9)$$

Integrating equation (9) from  $y = 0$  to  $y = h$  results in

$$\int_0^h \frac{\partial \bar{u}^2}{\partial x} dy + \int_0^h \frac{\partial \bar{u}\bar{v}}{\partial y} dy = \int_0^h -\frac{1}{\rho} \frac{\partial \bar{p}}{\partial x} dy - \int_0^h \frac{1}{\rho} \frac{\partial \overline{u'v'}}{\partial y} dy + g h \sin \alpha \quad (10)$$

Using Leibniz's rule equation (10) may be written as

$$\frac{d}{dx} \int_0^h \left[ \frac{\bar{u}^2}{g} + \frac{\bar{p}}{\gamma} \right] dy - h S_o + \frac{\tau_o}{\gamma} = 0 \quad (11)$$

where  $\tau_o = \left(-\overline{u'v'}\right)_o$  is the boundary shear stress and  $S_o$  is the bottom slope. Equation (11) may be rewritten as

$$\frac{dS}{dx} = h(S_o - S_f) \quad (12)$$

where  $S_f = \tau_o/(yh)$  is the friction slope and  $S$  is the specific momentum. Using equation (6) for the pressure distribution  $S$  is given by

$$S = \int_0^h \left[ \frac{\bar{u}^2}{g} + \frac{\bar{p}}{\gamma} \right] dy = \frac{h^2}{2} + \frac{q^2}{gh} \left( 1 + \frac{hh'' - h'^2}{3} \right) \quad (13)$$

Expanding the term  $dS/dx$  in equation (12), and integrating the result after elimination of the term  $h$  in the RHS of equation (12) yields

$$\frac{dH}{dx} = S_o - S_f \quad (14)$$

$H$  is the depth-averaged specific energy head. Using equation (6) for the pressure distribution  $H$  is given by

$$H = \frac{1}{h} \int_0^h \left[ \frac{\bar{u}^2 + \bar{v}^2}{2g} + \frac{\bar{p}}{\gamma} + y \cos \alpha \right] dy = h + \frac{q^2}{2gh^2} \left( 1 + \frac{2hh'' - h'^2}{3} \right) \quad (15)$$

Therefore, the depth-averaged mean energy balance is equivalent to the  $x$ -momentum balance. The system of equations (12) and (13) is fully equivalent to that of equations (14) and (15). Both energy and momentum considerations results in the same system of differential equations for  $h = h(x)$ .

### 3. Undular Hydraulic Jump

The undular hydraulic jump is a transitional free surface flow from supercritical,  $F > 1$ , to subcritical flow,  $F < 1$ , in the form of an undulating flow profile (Fig. 1). The flow pattern in the undular jump is complex and three-dimensional for  $F_1 > 1.2$ . In these conditions shockwaves appear in the upstream supercritical reach due to the boundary layer separation at channel sidewalls resulting from the adverse pressure gradient  $dh/dx > 0$ . These shockwaves (Fig. 1 a, b and c) create a 3D wavy free surface, with a recirculation pattern near the sidewalls (Fig. 1 c). The shockwave and sidewall boundary layer interaction results in local head losses, which are partially responsible of the spatial flow features. For  $F_1 < 1.2$  these effects are absent, and a perfect 2D free surface flow pattern is found in experiments (Fig. 1 d y e). Both cases of 2D and 3D flow patterns in undular jumps will be considered.

The results of the present model are compared below with the experimental data obtained by Chanson (1995). The experimental data for an undular jump of  $F_1 = 1.08$  (Test HCUJ10b) are presented in Fig. 2, using the critical depth  $h_c = (q^2/g)^{1/3}$  as the scaling. The system of ordinary differential equations (14) and (15) for the present theory was integrated for the unknowns  $h(x)$  and  $H(x)$  using a 4<sup>th</sup>-order Runge-Kutta method. The friction slope in equation (14) was estimated by the Darcy-Weisbach equation (Montes, 1998)

$$S_f = \frac{f}{4h} \frac{U^2}{2g} \quad (16)$$

where  $f$  is the friction factor. For turbulent smooth flow Haaland's equation (White, 1991)

$$f = \left[ -1.8 \log_{10} \left( \frac{6.9}{4R_1} \right) \right]^{-2} \tag{17}$$

was used. The approach flow Reynolds number is  $R_1 = q/\nu$ , with  $\nu$  as the kinematic viscosity. The accuracy of equation (17) is  $\pm 2\%$  compared to the Colebrook-White equation, i.e. it is adequate for practical purposes. The boundary conditions taken at the toe of the undular jump (subscript 1, Fig. 1 d) were  $h_1 = h(x = 0) = F_1^{-2/3}$ ,  $h'_1 = h'(x = 0) = 0$  and  $h''_1 = h''(x = 0) = 0$ . The value of  $H_1 = H(x = 0)$  is deduced from equation (15) with  $h' = h'' = 0$ . This set of boundary conditions implies a hydrostatic pressure distribution at  $x = 0$ .

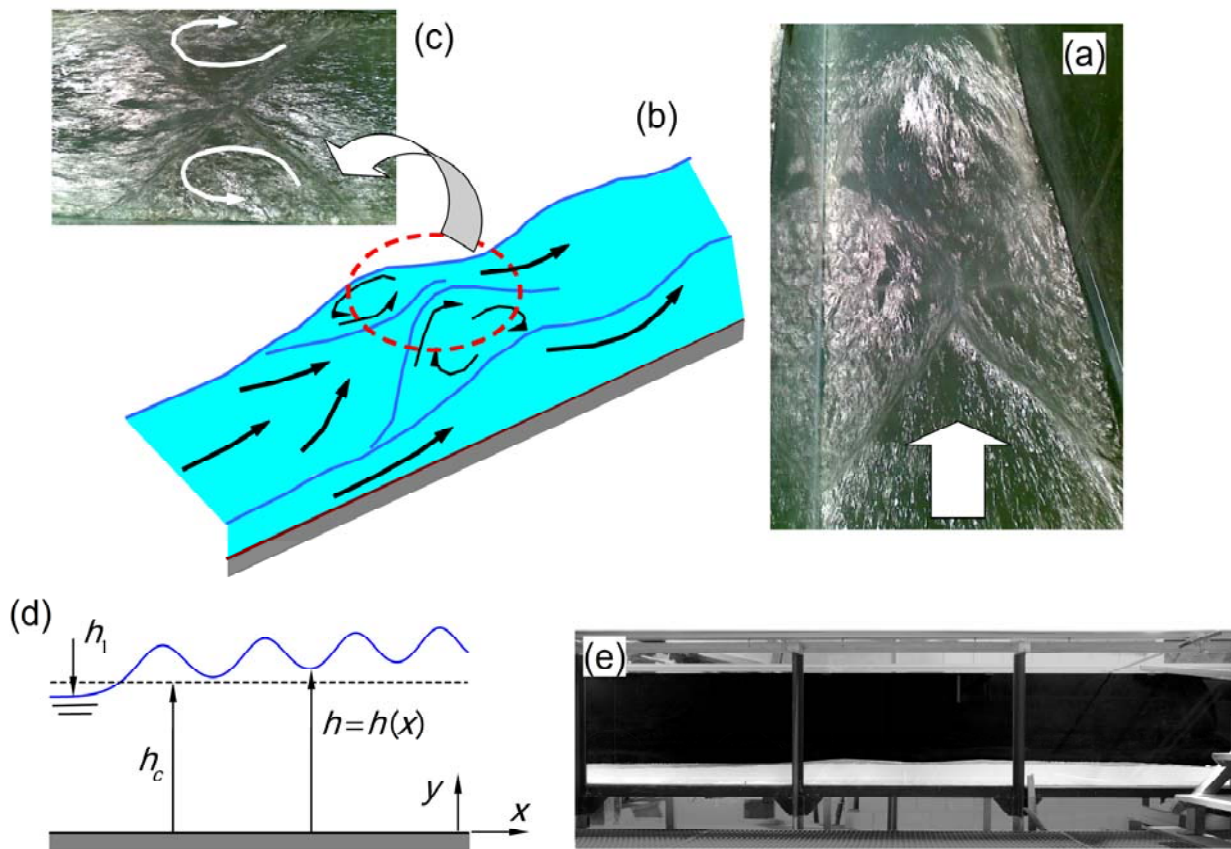


**Figure 1: The undular hydraulic jump (a) experiment with  $F_1 > 1.2$ , (b) typical 3D flow with shockwaves for  $F_1 > 1.2$ , (c) detail of shockwave intersection, (d) typical 2D flow surface with  $F_1 < 1.2$ , (e) experiment with  $F_1 < 1.2$**

The numerical results for  $F_1 = 1.08$  are shown in Fig. 2, revealing that the Boussinesq system, equations (14) and (15), with Haaland's equation for turbulent friction, reasonably predicts the wavy flow profile of the undular hydraulic jump. Maximum and minimum depth predictions at the wave crests and troughs compare well with the experiments, as well as wave amplitude and wave lengths.

It is still open the question whether the approximation adopted herein for the turbulence friction is reasonable or not. To further investigate this point, the detailed numerical computations done by Schneider et al. (2009) using a  $k-\epsilon$  model to integrate the complete

Reynolds equations for undular hydraulic jump flow are considered in Fig. 3 with experimental results for the same case. Note that the system of equations. (14) and (15) is the result of an approximate integration of the Reynolds equations. Thus, the accuracy of the present model will be checked against the complete integration of the Reynolds equations by Schneider et al. (2009).

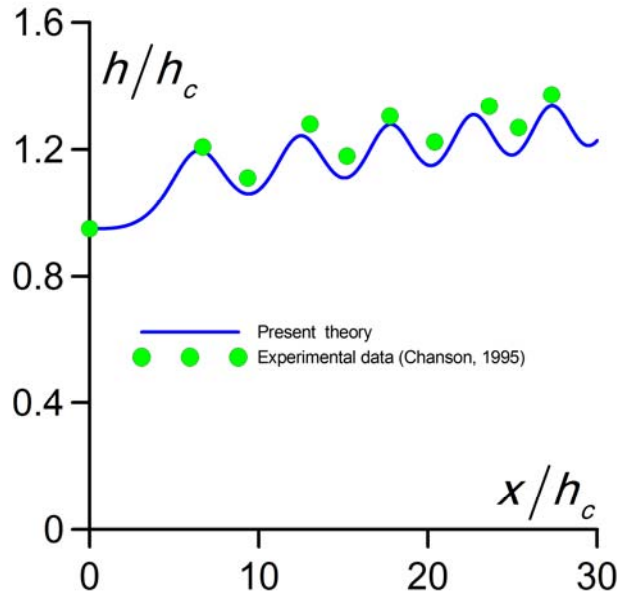


Figure 2: Undular hydraulic jump profile  $h/h_c(x/h_c)$  for  $F_1 = 1.08$ ,  $R_1 = 72727$ ,  $S_o = 0.004$

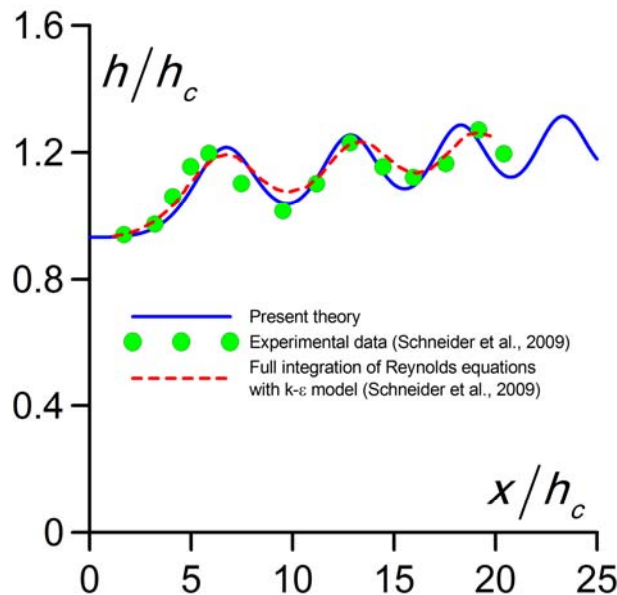


Figure 3: Undular hydraulic jump profile  $h/h_c(x/h_c)$  for  $F_1 = 1.11$ ,  $R_1 = 93000$ ,  $S_o = 1/282$

The simulation using the present 2D turbulent Boussinesq model is included in Fig. 3. It can be seen that the Boussinesq solution allowing for turbulent friction agrees very well with both experimental data and the numerical results of the integration of the complete Reynolds

equations. Thus, the approximation proposed herein is accurate, reasonably describing both the effects of friction and streamline curvature in undular hydraulic jumps.

Furthermore, an undular jump profile with  $F_1 = 1.36$  is considered in Fig. 4 to describe the flow features with shockwaves. Experimental data for the axial flow profile obtained by Hager and Hutter (1984) are plotted in Fig. 4 to compare with the model results. It can be seen that the model gives a good agreement with observations for the first wave profile. After the first wave, however, the computed wave amplitude is larger than that observed. This phenomenon may be explained in relation to the appearance of shockwaves (Fig. 1). The shockwave action causes a local head loss that is noticeable after the first wave crest, where the lateral shock-fronts intersect (Fig. 1 c). This additional head loss results in damped wave amplitude after the first crest, because the available energy head to maintain the cnoidal wave train diminishes. This feature is not predicted by computations allowing only for the bottom friction drag, which produces the larger wave amplitudes reported in Fig. 4. To verify this observation, after the first wave a second computation was done, starting at the inflexion point of the first crest. At this point the corresponding head loss was estimated from the experimental data. The results are included in Fig. 4, showing an excellent agreement for the downstream part of the flow profile. Therefore the 3D flow features are relevant for  $F_1 > 1.2$ , and the additional shock-wave energy loss determinates the downstream cnoidal wave profile after the first crest.

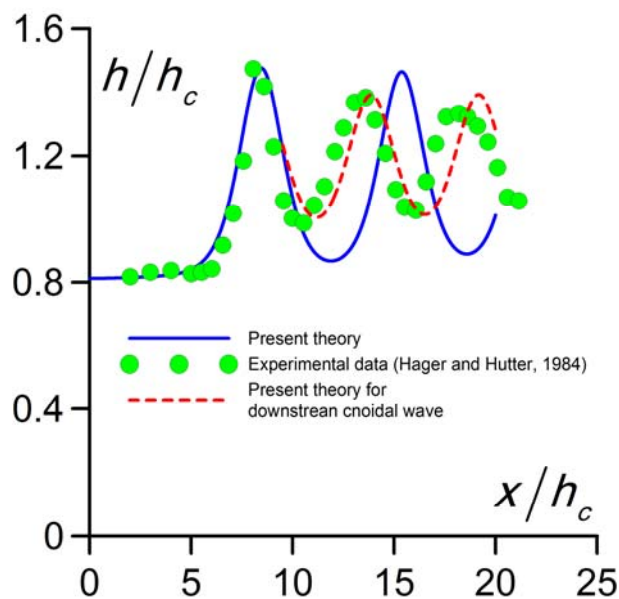


Figure 4: Undular hydraulic jump profile  $h/h_c(x/h_c)$  for  $F_1 = 1.36$ ,  $R_1 = 90000$ ,  $S_o = 0.0014$

#### 4. Undular Weir Flow

The undular weir flow is a transitional free surface flow from subcritical,  $F < 1$ , to supercritical flow,  $F > 1$ , in the form of an undulating flow profile. Undular flow over horizontal, rough broad-crested weir is considered in Fig. 5 (Serre, 1953; Montes, 1986). The upstream weir edge is rounded to avoid flow separation. Equations (14) and (15) were integrated numerically using a 4<sup>th</sup>-order Runge-Kutta method with  $H_o/h_c = 1.626$ , where  $H_o$  is the approach flow energy head. The boundary conditions used were the test data at the first wave trough  $h/h_c = 1.196$  and  $h' = 0$ . The friction slope  $dH/dx$  was determined using a Bazin roughness coefficient of 0.41 (Serre, 1953). The results for  $h = h(x)$  are compared with test data in Fig. 5, resulting in excellent agreement both for the wave crests and troughs.

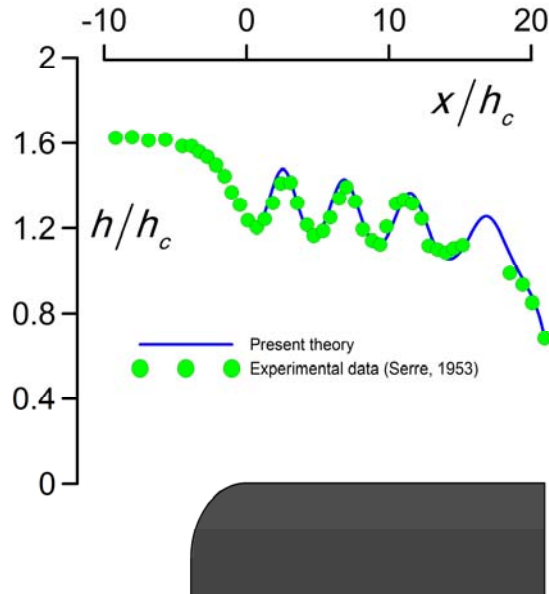


Figure 5: Undular weir flow profile  $h/h_c(x/h_c)$  for  $H_o/L = 0.078$

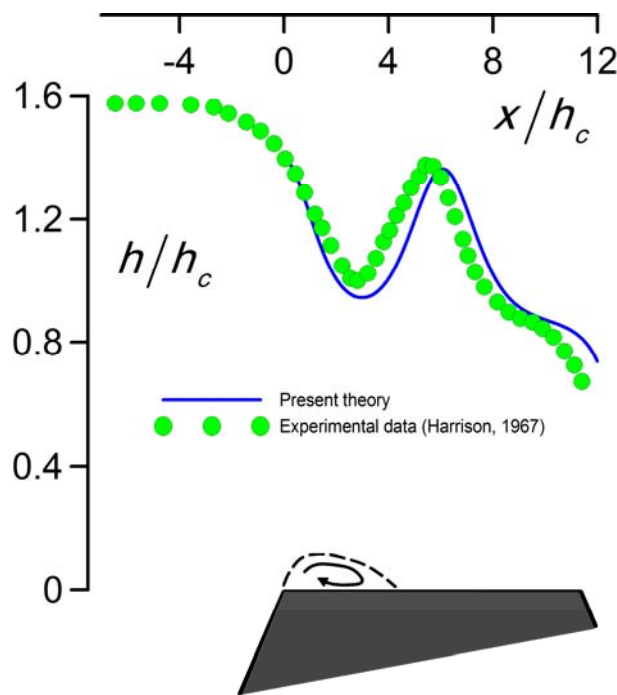


Figure 6: Undular weir flow profile  $h/h_c(x/h_c)$  for  $H_o/L = 0.136$ ,  $R_1 = 74500$

Further, the model predicts accurately the downstream boundary condition, corresponding to a free overfall. Another case is considered in Fig. 6 using the test data of a horizontal, smooth trapezoidal profile weir for  $H_o/L = 0.136$  (Harrison, 1967). The corresponding numerical simulation is also included, showing a fair concordance. Note that when  $H_o/L$  increases the flow profile of a broad-crested weir is still undular, but the wave train is damped to satisfy the boundary condition forced by the downstream slope break. This fact can be seen comparing the flow profiles in Figs. 5 and 6. In the test case of Fig. 6 there is only one



wave in the flow profile. The upstream slope break is associated with a separation bubble, not accounted for in the present model.

The limiting case of a cnoidal wave when the energy head drop below  $H/h_c = 1.5$  due to friction is the free overfall profile. The present model was applied to a horizontal free overfall in a hydraulically smooth channel with upstream critical flow conditions. The results are shown in Fig. 7. The initial point to start computation was taken as  $h/h_c(x/h_c = -5) = 1$ , corresponding to critical flow conditions  $F_1 = 1$ . The initial free surface slope was set to  $h' = -0.01$  and at this point  $H/h_c \approx 1.5$ . As shown in Fig. 7, the computation results are in excellent agreement with Hunter Rouse's experimental observations (Montes, 1998).

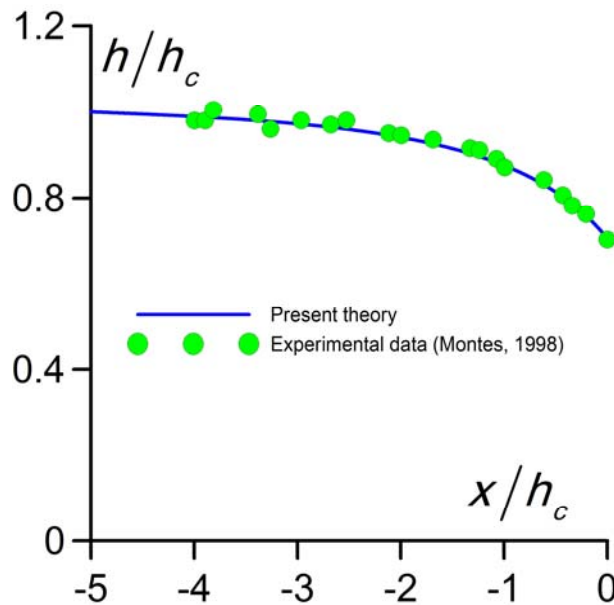


Figure 7: Free overfall profile  $h/h_c(x/h_c)$  for  $F_1 = 1$ ,  $R_1 = 90000$

## 5. Conclusions

In the present research two open channel flow types near the critical depth, the undular hydraulic jump and the undular weir flow, were studied based on a Boussinesq-type energy equation allowing for friction effects, obtained from the approximate integration of the Reynolds equations for turbulent flow.

The results of the present approach for the undular hydraulic jump compare well with experimental data. Also, the model results were similar to those obtained through the integration of the complete Reynolds equations for turbulent flow in an undular hydraulic jump. This confirms that the present model describes well 2D turbulent free surface flows with significant streamline curvature. The model was applied to undular weir flow over broad-crested weirs as well, and the results were close to the experimental observations. Therefore the proposed model can be safely used for the description of the operational conditions of broad-crested weirs.

Based on the agreement obtained between theory and experiments the advanced hydraulic modelling approach can be proposed for the hydraulic analysis of free surface flows across the critical depth, where standard hydraulic computations based on the gradually varied flow theory fails. As an additional consequence, the use of standard solutions in engineering problems must be carefully explored to avoid unexpected unreal results.

## 6. Notation

$F$  = Froude number (-)

$f$  = friction factor (-)

$g$  = acceleration of gravity ( $\text{m/s}^2$ )

$H$  = depth-averaged specific energy head (m)

$h$  = flow depth normal to channel bottom (m)

$y$  = distance normal to channel bottom (m)

$\bar{p}$  = time-averaged pressure ( $\text{N/m}^2$ )

$q$  = unit discharge ( $\text{m}^2/\text{s}$ )

$L$  = crest length (m)

$R$  = Reynolds number (-)

$S_f$  = friction slope (-)

$S_o$  = bottom slope (-)

$S$  = specific momentum ( $\text{m}^2$ )

$\bar{u}$  = time-averaged turbulent velocity parallel to bottom (m/s)

$U$  = depth-averaged flow velocity (m/s)

$\bar{v}$  = time-averaged turbulent velocity normal to bottom (m/s)

$x$  = streamwise distance (m)

$\alpha$  = angle of bottom with horizontal (rad)

$\rho$  = fluid density ( $\text{N/m}^3$ )

$\gamma$  = specific weight ( $\text{N/m}^3$ )

$\eta$  = dimensionless distance normal to channel bottom (-)

$\tau$  = Reynolds stress ( $\text{N/m}^2$ )

$\tau_o$  = boundary shear stress ( $\text{N/m}^2$ )

$\nu$  = kinematic viscosity ( $\text{m}^2/\text{s}$ )

### *Subscripts*

1      approach flow

c      critical flow

## 7. Acknowledgements

The first Author was supported by a contract of modality JAE-DOC of the program "Junta para la Ampliación de Estudios", CSIC, National Research Council of Spain, co-financed by the FSE.

## References

- Castro-Orgaz, O. (2009). Steady open channel flows with curved streamlines: The Fawer approach revised. *Env. Fluid Mech.* doi: 10.1007/s10652-009-9157-0.
- Chanson, H. (1995). *Flow characteristics of undular hydraulic jumps: Comparison with near-critical flows*. Res. Rep. CH45/95. Dept. Civ. Engng., University of Queensland, Brisbane, Australia.
- Chanson, H. (1996). Free surface flows with near critical flow conditions. *Can. J. Civ. Engng.*, 23(6), 1272-1284.
- Fawer, C. (1937). *Etude de quelques écoulements permanents à filets courbes*. Thesis, Université de Lausanne. La Concorde, Lausanne, Switzerland.
- Hager, W.H. & Hutter, K. (1984). On pseudo-uniform flow in open channel hydraulics. *Acta Mech.*, 53(3-4), 183-200.
- Harrison, A. J. M. (1967). The streamlined broad crested weir. *Proceedings of the Institution of Civil Engineers*, London, England, 38(4), 657-678; 1969, 42(4), 575-599.
- Iwasa, Y. (1955). Undular jump and its limiting conditions for existence. *Proc. 5<sup>th</sup> Japan Natl. Congress Applied Mech.*, II-14 (pp. 315-319).
- Mandrup-Andersen, V. (1978). Undular hydraulic jump. *J. Hydraul. Div. ASCE*, 104(HY8), 1185-1188; Discussion: 105(HY9), 1208-1211.
- Marchi, E. (1963). Contributo allo studio del risalto ondulato. *Giornale del Genio Civile*, 101(9), 466-476.
- Matthew, G. D. (1963). On the influence of curvature, surface tension and viscosity on flow over round-crested weirs. *Proceedings of the Institution of Civil Engineers*, London, England, 25(4), 511-524. Discussion: 1964, 28(4), 557-569.
- Matthew, G. D. (1991). Higher order, one-dimensional equations of potential flow in open channels. *Proceedings of the Institution of Civil Engineers*, London, England, 91(2), 187-201.
- Montes, J.S. (1986). A study of the undular jump profile. 9<sup>th</sup> *Australasian Fluid Mech. Conf.* (pp.148-151). Auckland.
- Montes, J.S. (1998). *Hydraulics of open channel flow*. Reston VA: ASCE Press.
- Montes, J. S. & Chanson, H. (1998). Characteristics of undular hydraulic jumps: Results and analysis. *J. Hydraul. Engng.*, 124 (2), 192-205.
- Schneider, W., Jurisits, R. & Bae, Y.S. (2009). An asymptotic iteration method for the numerical analysis of near-critical free-surface flows. 14<sup>th</sup> *International conference on fluid flow technologies: Conference on modelling fluid flow* (8 pages). Budapest.
- Serre, F. (1953). Contribution à l'étude des écoulements permanents et variables dans les canaux. *La Houille Blanche*, 8(6-7), 374-388; 8(12), 830-887.
- White, F.M. (1991). *Viscous fluid flow*. New York: McGraw-Hill.

### Correspondencia (Para más información contacte con):

José Luis Ayuso Muñoz  
Professor, Dept. of Rural Engineering, University of Cordoba, Da Vinci Bldg., Cra Madrid km 396,  
14071 Cordoba, Spain, e-mail:  
E-mail : ir1aymuj@uco.es